Biomaterial Resorption Rate and Healing Site Morphology of Inorganic Bovine Bone and β-Tricalcium Phosphate in the Canine: A 24-month Longitudinal Histologic Study and Morphometric Analysis

Zvi Artzi, DMD[1]/Miron Weinreb, DMD[2]/Navot Givol, DMD[3]/Michael D. Rohrer, DDS, MS[4]/
Carlos E. Nemcovsky, DMD[1]/Hari S. Prasad, BS, MDT[5]/Haim Tal, DMD, PhD[6]

Purpose: *An inorganic xenograft (inorganic bovine bone [IBB]) and a porous alloplast (β-tricalcium phosphate [β-TCP]) material were compared at different healing periods in experimental bone defects in dogs.* ***Materials and Methods:*** *Six round defects, 5 × 4 mm, were made on the lateral bony mandibular angle in 8 dogs at different times. Two defects were randomly filled with IBB, 2 with β-TCP, and 2 were left to blood clot. A bi-layer collagen membrane covered 1 defect of each type. Four specimens per treatment group were obtained for each treatment group at 3, 6, 12, and 24 months postoperatively. Morphometric analysis of decalcified (Donath technique) histologic slides was conducted using the measured areas of regenerated bone, grafted particles, and remaining concavity.* ***Results:*** *In IBB sites, complete bone healing was evident at 12 and 24 months, but grafted particles dominated the sites. In β-TCP sites, only particle remnants remained at 12 months. At 24 months, particles had completely resorbed in both membrane-protected (MP) and uncovered (UC) defects. Data were combined for final analysis since there were no statistically significant differences within each graft material group (MP or UC). Mean bone area fraction increased from 3 to 24 months at all sites. In bone area fraction a statistically significant difference was found between 3 and 6 months in the IBB and β-TCP groups. IBB sites also showed such significance between 6 and 12 months. A statistically significant difference was found between MP ungrafted sites (42.9%) vs IBB (24.7%) and vs the control (24.8%) at 3 months. At 6 months, β-TCP bone area fraction (68.8%) was significantly greater than IBB (47.9%) and control (37.5%) sites. At 12 months, β-TCP bone area fraction (79.0%) was significantly greater than the control (42.5%). At 24 months, β-TCP bone area fraction (86.5%) was significantly greater than IBB (55.6%) sites. Mean particle area fraction of β-TCP sites decreased gradually until complete resorption at 24 months. IBB sites showed a significant decrease only between 3 (38.7%) and 6 (29.4%) months.* ***Discussion and Conclusion:*** *Complete bone healing was established in all grafted defects. IBB and β-TCP are both excellent biocompatible materials. However, at 24 months β-TCP particles were completely resorbed, whereas IBB particles still occupied a remarkable area fraction without significant resorption beyond 6 months.* (More than 50 references.) INT J ORAL MAXILLOFAC IMPLANTS 2004;19:357–368

Key words: *alloplast, β-tricalcium phosphate, biomaterial resorption, bovine bone mineral, osteoconduction, xenograft*

[1]Senior Lecturer, Department of Periodontology, The Maurice and Gabriela Goldschleger School of Dental Medicine, Tel Aviv University, Tel Aviv, Israel.
[2]Associate Professor, Department of Oral Biology, The Maurice and Gabriela Goldschleger School of Dental Medicine, Tel Aviv University, Tel Aviv, Israel.
[3]Attending Surgeon, Department of Oral and Maxillofacial Surgery, Chaim Sheba Medical Center, Tel Hashomer, Israel.
[4]Professor, Division of Oral & Maxillofacial Pathology, School of Dentistry, University of Minnesota, Minneapolis, Minnesota.
[5]Research Scientist, Hard Tissue Research Laboratory, School of Dentistry, University of Minnesota, Minneapolis, Minnesota.
[6]Professor, Department of Periodontology, The Maurice and Gabriela Goldschleger School of Dental Medicine, Tel Aviv University, Tel Aviv, Israel.

Natural and synthetic bone substitutes, when used in bone regeneration procedures associated with implant placement, should comply with several criteria. These include biocompatibility, osteoconductivity, and complete lack of antigenicity. The material should serve as a scaffold for capillary ingrowth. Complete resorption of the material, which is to be replaced by new osseous tissue at a

Correspondence to: Dr Zvi Artzi, Department of Periodontology, The Maurice and Gabriela Goldschleger School of Dental Medicine, Tel Aviv University, Tel Aviv, Israel. Fax: +972 3 6409250. E-mail: zviartzi@post.tau.ac.il

later stage, is preferable. The grafting agent serves as both a mechanical support for the overlying barrier membrane and an osseoinductive or osseoconductive matrix for the regenerating tissue.

Several bone derivatives or substitutes have been used in bone reconstruction. Allografts, xenografts, and alloplasts are the 3 major nonautologous graft sources. Bovine bone mineral, a xenograft, and β-tricalcium phosphate (β-TCP), an alloplast, are both excellent biocompatible materials. Inorganic bovine bone (IBB) has been extensively investigated and has produced satisfactory results in correcting alveolar ridge deficiencies[1–7] as well as in peri-implant repair.[8–10] It has also been applied in socket preservation techniques[11–14] and is considered 1 of the preferred nonautologous graft materials in sinus augmentation procedures.[10,15–20] It has been speculated that the preservation of delicate porotic morphology during sterilization probably enhances the effectiveness of this material.[21,22]

Similar findings have been attributed to β-TCP.[23,24] It is also biocompatible[25–27] and acts as a space maker and scaffold for bone ingrowth.[28–32] In a comparative histomorphometric study on different biomaterials in miniature pigs,[33] TCP showed the most promising results for biodegradation and substitution among other nonautologous graft materials such as coral-derived hydroxyapatite and demineralized freeze-dried bone allografts. IBB was not tested.

However, neither IBB nor β-TCP have achieved the level of osteoconductivity or the resorption rate necessary for absolute general acceptance. The purpose of this study was to compare the potential of IBB and β-TCP to promote bone regeneration in experimental bone defects in dogs. (The rate of bone formation coincides with the rate of graft material resorption.) The surface morphology of the graft sites after different healing periods was evaluated morphometrically.

MATERIALS AND METHODS

The study sample consisted of 8 mongrel dogs, 5 to 6 years old, weighing between 17 and 29 kg (average 21.6 kg). Premedication (2% Chanazine [Chanelle Veterinary, Loughrea, Ireland] and 20 mg/kg penicillin G benzathine [Durabiotic; Biochemie, Kundl, Austria]) was administered 30 minutes before the intravenous administration of the general anesthetic agent (20 mg/kg pentobarbital sodium). A facial incision was made using an electrosurgical device (SSE21; Valleylab, Boulder, CO) and a knife with a no. 15 blade to expose the outer (lateral) line angle of the mandible. For homeostasis and to reduce postoperative pain, 2% lidocaine with norepinephrine (1:100,000) was administered by local infiltration. The mandibular bone surface was exposed from the mental foramen anteriorly to the ramus notch posteriorly.

To make the defects, a grid with 6 round holes was applied to the bony plate slightly inferior to the estimated location of the mandibular canal pathway (Fig 1a). Six round defects, each 5 mm in diameter and 4 mm deep, were prepared at least 3 mm apart using an inverted-cone diamond bur mounted on a high-speed hand drill. The dimensions of the defects were verified with a periodontal probe. In each dog, 2 randomly selected defects were filled with IBB particles (Bio-Oss; Geistlich Biomaterials, Wolhusen, Switzerland) and 2 with β-TCP (Cerasorb; Curasan, Kleinstheim, Germany). The remaining 2 defects were left ungrafted to form a blood clot. Three defects (1 of each type) were covered with an absorbable collagen membrane (Bio-Gide, Geistlich Biomaterials) as a guided tissue regeneration (GTR) barrier, and stabilized with 1.6-mm miniscrews (Auto-Drive; OsteoMed, Addison, TX) (Fig 1b). In each dog, a membrane-protected, ungrafted defect and an unprotected, ungrafted defect served as controls for the membrane-protected grafted defects and the uncovered grafted defects, respectively. Soft tissue closure was performed in layers; the inner muscles were sutured with 4-0 chromic catgut suture (Johnson & Johnson/Ethicon, Cornelia, GA) and the outer skin with 4-0 resorbable rapid, Vicryl polyglactin sutures (Johnson & Johnson/Ethicon).

This procedure was repeated on the contralateral side at a different given time; thus each dog had 2 sets of defects that were allowed to heal for periods of different lengths (eg, 3 and 6 months, 6 and 12 months, 3 and 24 months). Ninety-six defects (6 defects × 2 sides × 8 dogs) were made—4 defects per defect type per healing period. Defects were allowed to heal for either 3, 6, 12, or 24 months. Postoperative medication included an intramuscular injection of antibiotics (240,000 IU/mL Durabiotic). The dogs were fed a soft diet for 2 weeks. The wound healing site was observed daily for the first week, then weekly for the first month.

Four biopsy specimens were obtained for each healing period. The dogs were sacrificed using 2% Chanazine as premedication followed by a lethal dose of sodium pentobarbital injected intravenously. Subsequently, 300 mL of 10% neutral buffered formalin was injected into the external carotid artery branch[34] to achieve tissue fixation prior to specimen block removal.

Fig 1a Six round defects, 5 × 4 mm, were made on the buccal bony shelf of the mandible.

Fig 1b Membrane-protected defects and an uncovered defect before soft tissue suturing.

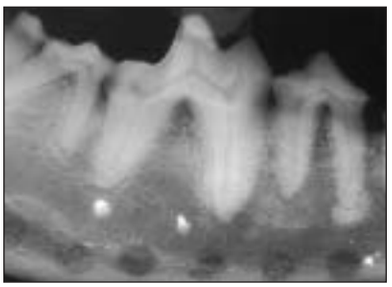

Fig 1c A specimen block radiograph in which defect radiolucency is evident.

Radiographs of the specimen blocks were taken prior to histologic processing. The outlined defects were distinguishable at the inferior mandibular border (Fig 1c).

Histologic Preparation

The specimen blocks were placed in 10% neutral buffered formalin, divided in half through the area of interest, and immediately dehydrated with a graded series of alcohols for 9 days. After dehydration, the specimens were infiltrated with a light-polymerized embedding resin (Technovit 7200 VLC, Heraeus Kulzer, Hanau, Germany). After 20 days of infiltration with constant shaking at a normal atmospheric pressure, the specimens were embedded and polymerized by 450-nm light at a temperature of 40°C. The specimens were then prepared using the cutting/grinding method described by Donath and Breuner.[35–37] They were cut to a thickness of 150 µm on an EXAKT cutting/grinding system (EXAKT Technologies, Oklahoma City, OK). Slides were polished to a thickness of 40 µm using the EXAKT microgrinding system followed by alumina polishing paste and stained with Stevenel's blue and Van Gieson's picro fuchsin. Photomicrographs were obtained using a Zeiss Axiolab photomicroscope (Carl Zeiss Microimaging, Thornwood, NJ).

Histomorphometry

A projection microscope (Visopan; Reichert, Leica, Vienna, Austria) was used for morphometric measurements (×20 final magnification). A 64-square (1.5 cm × 1.5 cm) graticule was superimposed on the screen for the point-counting calculation.[13,20,38,39] All measurements were taken by the same investigator (ZA). To determine the reproducibility of the measurements and the coefficient of variation for each parameter, 10 randomly selected slides were measured 5 times, not consecutively, without reference to the previous data. The mean coefficients of variation of bone, biomaterial particle, and remaining concavity area fractions were 2.2%, 1.9%, and 1.8%, respectively, indicating that these measurements were highly reproducible. Prior to measuring, the exact original boundaries of each defect were determined. If necessary, polarized light microscopy, which easily distinguished between the newly formed bone and the native bone, was used. In most examined section cuts, the defect boundaries were identified without polarized light.

Whenever the graticule-square center (marked by a "+") hit one of the components, regenerated bone or a grafted particle, the specific component scored 1 point. The sum of the points overlying each specified component (Pi) was calculated. The area of each component was calculated as a percentage, or fraction, of the whole section area—$Pi/\Sigma i$, where Σi represents the total number of points superimposed on each section.

Additionally, the morphologic outcome of the defect was quantitated by counting the number of graticule-square center points found on the external area(s) beyond the periosteum devoid of graft particles or regenerated bone to represent the residual concavity (RC) area fraction.

Statistical Analysis

To evaluate the relatively small sample size (n = 4) of each defect type at each healing period, 2 statistical analyses were conducted: the nonparametric Kruskal-Wallis 1-way analysis of variance for ranking differences of means and for multiple comparisons within each healing period, and the nonparametric Mann-Whitney test for multiple comparisons within each examined site between each pair of consecutive periods. BMDP statistical software was used for the statistical analyses (SPSS, Chicago, IL). This test was also applied to the particle area fraction comparison of the 2 graft materials at each healing period. The Bonferroni method was used to adjust for multiple testing for comparisons among treatment groups and for comparisons across time periods. The level of significance was set at $P \leq .05$.

Fig 2 At 3 months, newly formed bone surrounded part of the grafted IBB particles, mainly close to the native bony walls (Stevenel's blue and Van Gieson's picro fuchsin; original magnification ×20).

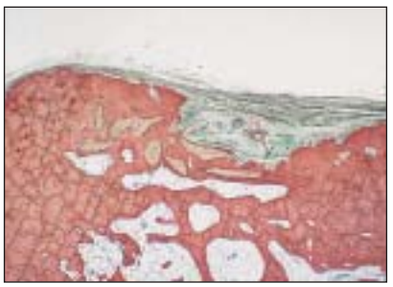

Fig 3a At 6 months, most of the defects were filled with newly formed bone incorporated around the grafted particles (Stevenel's blue and Van Gieson's picro fuchsin; original magnification ×20).

Fig 3b Multinucleated cells, ie, osteoclasts, near the grafted IBB particles (Stevenel's blue and Van Gieson's picro fuchsin; original magnification ×400).

RESULTS

Histologic Observations

IBB Sites. Membrane-protected and unprotected grafted sites showed similar findings. At 3 months, IBB particles filled the defect. Newly formed bone was evident near the bony walls, occasionally surrounding some of the grafted particles at the peripheral zone (Fig 2). The newly formed bone observed in the defect center, away from the bony walls, was primarily surrounded by the particles. There was an abrupt transition from the well-organized old bone to the highly cellular newly formed bone. At 6 months, most of the particles were surrounded by newly formed bone. The particles were about the same size as they had been at 3 months. The newly formed bone showed a tendency to bridge the defect; however, at this stage of healing, a significant soft tissue concavity was still observed (Fig 3a). Particles not surrounded by bone were layered by greenish striae staining, showing osteoid formation. Xenograft resorption was not a typical finding, and multinucleated cells, ie, osteoclasts, were seldom seen near the particles (Fig 3b).

At 12 and 24 months, the grafted defects showed complete bone healing; the defect configuration had been completely eliminated (Fig 4a). Although the newly formed bone was mature and organized at this stage, the defect boundaries and regenerated bone were clearly distinguishable by the staining and tissue arrangement. The regenerated bone included haversian canals, ie, osteons, in accordance with the grafted particles' configuration (Fig 4b).

β-TCP Sites. At 3 months, β-TCP particles were aggregated in the defects. Some were incorporated with the newly formed bone, particularly on the periphery of the sites. While the uncovered β-TCP grafted defects showed newly formed bone primarily in the defect base, close to the bony walls (Fig 5a), the membrane-protected defects showed superficially more regenerated bone mass (Fig 5b). Nevertheless, both membrane-protected and uncovered sites exhibited a remarkably concave healing configuration at this stage. Higher magnification of the β-TCP particles, which were surrounded by newly formed bone, showed grafted particles in advancing stages of resorption (Fig 5c). In the defect center, where no bone was observed, greenish-stained osteoid formations encapsulated the particles (Fig 5d), identical to the IBB particles in the early healing stage.

At 6 months, β-TCP–grafted defects were almost completely filled with bone (Fig 6). The grafted particles were completely embedded in the newly formed regenerated bone. At 12 months, the membrane-protected β-TCP site showed complete bridging of the defect; remnants of the grafted particles were still evident in the center of the defect surface, completely surrounded by the regenerated bone (Fig 7). The uncovered sites showed similar progress. The newly formed bone was still easily distinguished from the surrounding well-organized native bone. In polarized microscopy, the remodeled regenerated bone was well defined by its brightness compared to the dark native bone.

At 24 months, the configuration of the sites was consistent with complete healing (Fig 8). In polarized microscopy, the bone, although organized, had not reached final maturation. The new bone could be distinguished with staining and by its tissue organization. The β-TCP particles had been completely resorbed and replaced by established organized bone. However, a minor RC could still be seen.

Ungrafted Sites. At 3 months, newly formed bone was observed near the native bony walls and under the membrane at the membrane-protected ungrafted site (Fig 9a). Continual healing with the same pattern was observed at 6, 12, and 24 months. At 24 months, the configuration of the membrane-protected defect showed complete bone healing (Fig 9b). However, the density of the regenerated bone appeared sparse compared to the grafted sites.

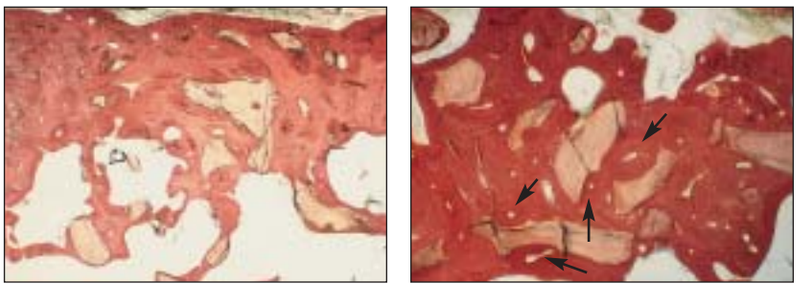

Fig 4a *(Left)* At 24 months, IBB particles dominated the sites and were completely incorporated with the newly formed bone to achieve complete healing site configuration (Stevenel's blue and Van Gieson's picro fuchsin; original magnification ×20).

Fig 4b *(Right)* Haversian canals, ie, osteons *(arrows),* established around IBB particles toward bone maturation (Stevenel's blue and Van Gieson's picro fuchsin; original magnification ×40).

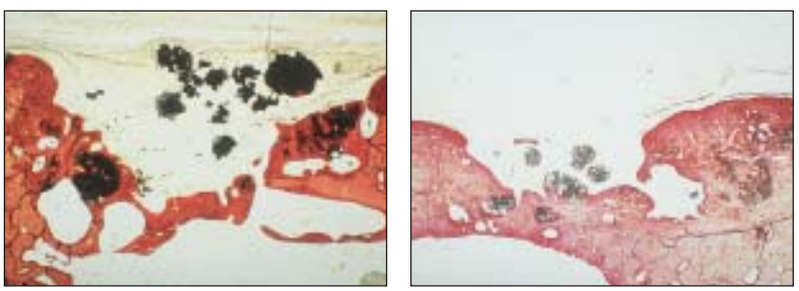

Fig 5a *(Left)* β-TCP uncovered site at 3 months. Newly formed bone was noticed near native bone surrounding some of the grafted particles (Stevenel's blue and Van Gieson's picro fuchsin; original magnification ×20).

Fig 5b *(Right)* β-TCP membrane-protected site at 3 months. Newly formed bone was seen close to native walls, attempting to re-establish under the membrane (Stevenel's blue and Van Gieson's picro fuchsin; original magnification ×20).

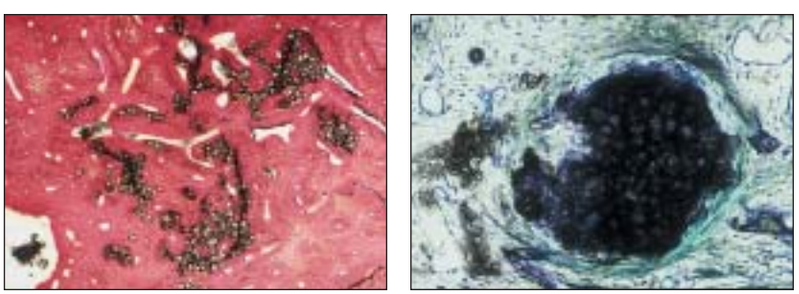

Fig 5c *(Left)* Newly formed bone incorporated with the grafted β-TCP particles that were in an advanced stage of resorption (Stevenel's blue and Van Gieson's picro fuchsin; original magnification ×100).

Fig 5d *(Right)* Greenish-stained osteoid formation was evident around β-TCP particles in the defect center (Stevenel's blue and Van Gieson's picro fuchsin; original magnification ×400).

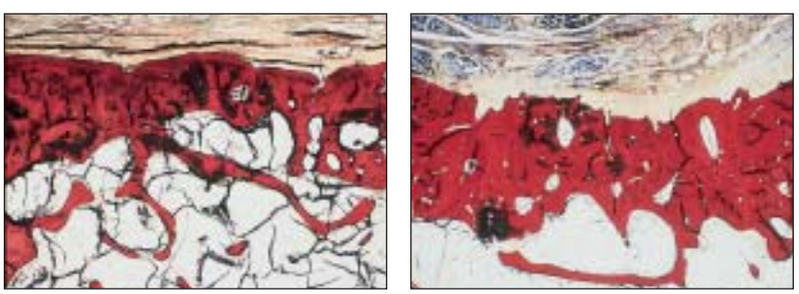

Fig 6 *(Left)* At 6 months, newly formed bone completely bridged the defect (Stevenel's blue and Van Gieson's picro fuchsin; original magnification ×20).

Fig 7 *(Right)* At 12 months only a few fragments of grafted β-TCP particles were present (Stevenel's blue and Van Gieson's picro fuchsin; original magnification ×20).

The uncovered blood-clotted sites (control) showed newly formed bone at the defect base. However, most of the defect was filled with connective tissue, presenting a remarkable concavity (Fig 10a). At 6, 12, and 24 months, the size of the defect decreased progressively along with bone remodeling. At 24 months, a superficial RC was observed (Fig 10b).

Morphometric Observations

Kruskal-Wallis ranking means showed an overall significant difference ($P < .05$) in bone, particle and RC area fractions at the different experimental sites. Since no significant difference was found between membrane-protected and uncovered grafted sites for any biomaterial at any healing period for any parameter (Tables 1 to 3), data were combined for a statistical analysis re-run.

Bone. Effect of Time. Mean bone area fraction gradually increased at both the grafted and ungrafted sites (Table 1). The β-TCP sites increased from 35.6% at 3 months to 86.5% at 24 months. They showed greater bone area fraction than the IBB sites in all examined healing periods. However, between consecutive periods a statistically significant difference was found only between 3 and 6 months ($P = .003$).

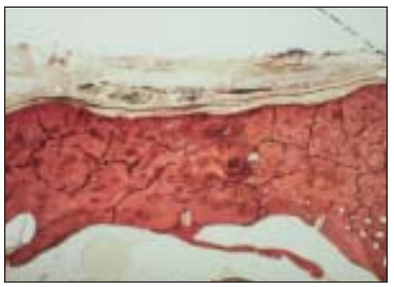

Fig 8 At 24 months, β-TCP particles were fully resorbed and the defect was completely filled by newly formed bone (Stevenel's blue and Van Gieson's picro fuchsin; original magnification ×20).

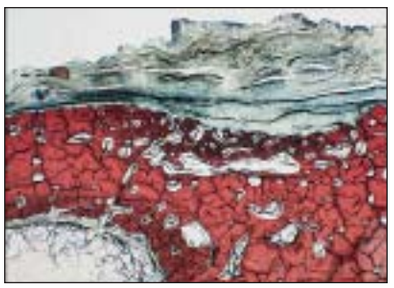

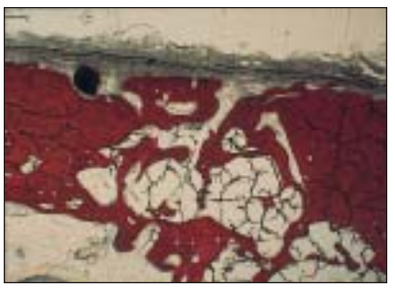

Fig 9a *(Left)* Newly formed bone established under the membrane at an ungrafted site at 3 months (Stevenel's blue and Van Gieson's picro fuchsin; original magnification ×20).

Fig 9b *(Right)* At 24 months complete bone healing was evident at the membrane-protected ungrafted site. Part of the fixation screw can be seen in black stain (Stevenel's blue and Van Gieson's picro fuchsin; original magnification ×20).

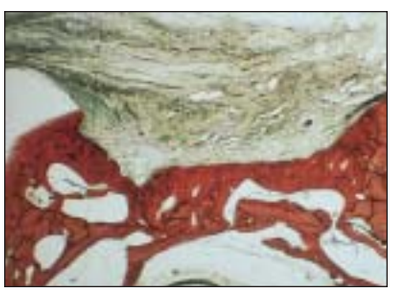

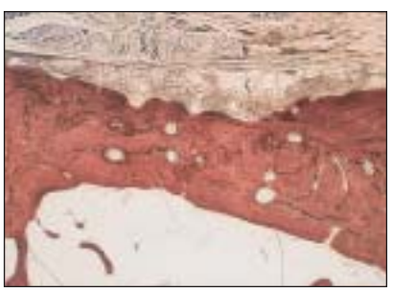

Fig 10a *(Left)* A remarkable concavity was evident at 3 months at the ungrafted uncovered site. Newly formed bone *(dark red)* was established only along the native bone walls (Stevenel's blue and Van Gieson's picro fuchsin; original magnification ×20).

Fig 10b *(Right)* The ungrafted uncovered site at 24 months. The remodeled bone occupied most of the site but a residual concavity was still evident (Stevenel's blue and Van Gieson's picro fuchsin; original magnification ×20).

Mean bone area fraction of IBB sites increased from 24.7% at 3 months to 55.6% at 24 months. Between consecutive periods, a statistically significant difference was found between 3 and 6 months ($P = .003$) and between 6 and 12 months ($P = .006$).

Effect of Biomaterial. Multiple comparisons of newly formed bone at 3 months revealed a significantly smaller bone area fraction at IBB and uncovered ungrafted sites versus the membrane-protected ungrafted sites. At 6 months, bone area fraction at the β-TCP sites was significantly greater than at the IBB and uncovered ungrafted sites. At 12 months, β-TCP sites no longer had significantly greater mean bone area fraction than IBB sites, but they did have significantly greater mean bone than uncovered ungrafted sites. At 24 months, β-TCP sites again had significantly greater bone area than IBB sites.

Biomaterial Particles. Effect of Time. Biomaterial particle area fractions at 3, 6, 12, and 24 months are presented in Table 2. The average β-TCP particle area fraction decreased from 27.1% at 3 months to 0% at 24 months, ie, all β-TCP particles were completely resorbed. A statistically significant reduction was found between 3 and 6 months ($P = .009$) and between 12 and 24 months ($P = .003$). IBB sites showed a slight decrease in particle area fraction from 38.7% at 3 months to 30.2% at 24 months. Nevertheless, a statistically significant difference was noted between 3 and 6 months ($P = .009$).

Effect of Biomaterial. Between the 2 different biomaterials, differences regarding average particle area fraction reached statistical significance at all healing periods (β-TCP < IBB).

Surface Site Morphology. Effect of Time. While all test sites showed a gradual decrease of RC area fraction toward complete bone fill, the uncovered ungrafted control sites showed the greatest residual area (31.8%) at 24 months (Table 3). Within the grafted sites, a significant decrease was found between 3 and 6 months ($P = .006$) and between 6 and 12 months ($P = .027$) at β-TCP sites, whereas at the IBB sites, RC area fraction decreased significantly between all consecutive periods.

Table 1 Percentage of Mean Bone Area Fraction at 3 to 24 Months

	Healing period (mo)							
	3		6		12		24	
	%	SE	%	SE	%	SE	%	SE
β-TCP								
UC	32.5	1.4	62.9	2.0	80.9	2.0	83.9	1.7
MP	38.7	2.9	74.7	4.4	77.1	3.7	89.1	3.1
Mean	35.6	1.9*	68.8	3.2	79.0	2.1	86.5	1.9
IBB								
UC	23.1	2.4	44.0	2.9	63.4	1.7	58.8	0.9
MP	26.4	3.8	51.7	2.5	61.2	4.3	52.4	1.7
Mean	24.7	2.2*	47.9	2.3*	62.3	2.2	55.6	1.5
Ungrafted control								
UC	24.8	3.7	37.5	1.5	42.5	3.7	60.9	1.1
MP	42.9	1.0	59.9	3.7	61.2	3.7	69.5	1.3
Statistical significance	IBB < $Cont_{MP}$ $Cont_{MP}$ > $Cont_{UC}$		β-TCP > IBB β-TCP > $Cont_{UC}$		β-TCP > $Cont_{UC}$		β-TCP > IBB	

β-TCP = β-tricalcium phosphate; IBB = inorganic bovine bone; MP = membrane protected; UC = uncovered; $Cont_{MP}$ = membrane-protected ungrafted control; $Cont_{UC}$ = uncovered ungrafted control; SE = standard error.
*P = .003.

Table 2 Percentage of Average Particle Area Fraction at 3 to 24 Months

	Healing period (mo)							
	3		6		12		24	
	%	SE	%	SE	%	SE	%	SE
β-TCP								
UC	24.8	4.8	16.2	1.6	8.1	1.9	0.0	0.0
MP	29.4	4.2	11.3	0.4	8.3	3.0	0.0	0.0
Mean	27.1	3.1†	13.8	1.2	8.2	1.7*	0.0	0.0
IBB								
UC	39.6	3.2	29.0	0.9	27.6	1.5	26.8	2.1
MP	37.9	2.1	29.8	3.5	26.8	2.2	33.7	3.6
Mean	38.7	1.8†	29.4	1.7	27.2	1.3	30.2	2.3
Statistical significance	β-TCP < IBB		β-TCP < IBB		β-TCP < IBB		β-TCP < IBB	

β-TCP = β-tricalcium phosphate; IBB = inorganic bovine bone; MP = membrane protected; UC = uncovered; SE = standard error.
*P = .003.
†P = .009.

Effect of Biomaterial. At 3 months, a statistically significant difference of multiple comparison between each site type of RC area fraction was found only between the ungrafted sites (RC area fraction was greater in uncovered sites than in membrane-protected sites). Between the grafted sites, a significant difference of RC area fraction was observed only at 6 months (β-TCP < IBB). At 6 and 12 months, β-TCP showed a significantly lower RC area fraction than the uncovered ungrafted control. IBB sites showed a significantly lower RC area fraction than the uncovered ungrafted control only at 12 and 24 months.

DISCUSSION

In the present animal model, both nonautogenous graft materials, IBB and β-TCP, demonstrated excellent biocompatibility and osteoconductivity. Newly formed bone surrounded the grafted particles 3 months after grafting. Osteoconductivity, as expressed by direct bone-to-particle contact, was primarily present at the IBB sites. Grafted particles not surrounded by newly formed bone were layered by greenish-stained osteoid formation. These particles were located mainly in the defect center, distal from the bony defect borders. Bone growth and

Table 3 Percentage of Mean Residual Concavity Area Fraction at 3 to 24 Months

	Healing period (mo)							
	3		6		12		24	
	%	SE	%	SE	%	SE	%	SE
β-TCP								
UC	54.2	11.0	17.3	3.3	7.0	2.6	3.9	0.6
MP	33.8	2.9	12.2	2.2	6.4	1.0	8.7	3.2
Mean	44.0	6.5†	14.8	2.1*	6.7	1.3	6.3	1.7
IBB								
UC	59.0	5.9	32.8	6.2	7.1	0.9	0.9	0.6
MP	48.2	2.7	27.4	4.6	7.7	1.9	1.3	1.3
Mean	53.6	3.6†	30.1	3.7‡	7.4	0.9‡	1.1	0.7
Ungrafted control								
UC	63.9	1.3	41.5	3.6	29.9	1.6	31.8	3.7
MP	32.1	3.9	24.7	2.9	9.6	2.2	6.8	2.8
Statistical significance	$Cont_{MP} < Cont_{UC}$		β-TCP < IBB β-TCP < $Cont_{UC}$		β-TCP < $Cont_{UC}$ IBB < $Cont_{UC}$		IBB < $Cont_{UC}$	

β-TCP = β-tricalcium phosphate; IBB = inorganic bovine bone; MP = membrane protected; UC = uncovered; $Cont_{MP}$ = membrane-protected ungrafted control; $Cont_{UC}$ = uncovered ungrafted control; SE = standard error.
*P = .027.
†P = .006.
‡P = .003.

maturation developed centripetally from the peripheral borders of the defect.

In the early periods of this study, ie, in the first 6 months, acceleration of bone formation was observed at the membrane-protected grafted sites, which was probably the result of the presence of the membrane. The GTR membrane serves as an osteoconductive factor and plays a significant role initially as an osteopromotive agent to the regenerated bone.[40,41] However, membrane-protected grafted defects did not reach a significantly greater amount of regeneration than the uncovered grafted ones at any healing period. Apparently, the application of a GTR membrane over these intrabony grafted sites was not significantly advantageous.

At 6 months, newly formed bone occupied most of the defects. It appears that the newly formed bone pathway actually buds itself through particle location, supporting the hypothesis that the high osteoconductivity of the grafted material encourages bone growth. Between 3 and 6 months bone area fraction progressively increased and was significantly greater at both β-TCP and IBB sites. Furthermore, bone area fraction at IBB sites also increased significantly between 6 and 12 months, which reflects the osteoconductivity of this material. At β-TCP sites, a significant difference was further observed only between 6 and 24 months. Membrane-protected ungrafted and uncovered ungrafted control sites continued to increase in bone area fraction, but the increases were insignificant statistically. Clinically, greater acceleration in the formation of new bone can be expected at sites grafted with IBB than at sites grafted with β-TCP site, as seen in the advanced healing phase, between 6 and 12 months.

A completely healed configuration could not be seen at either membrane-protected or uncovered grafted sites at 6 months. An RC was observed at all sites at 6 months. Nevertheless, grafted sites showed significantly lower RC area fraction versus controls, whether membrane-protected or uncovered. The change in the average RC area fraction was inversely related to the change in average bone area fraction; a significant decrease was observed between 3 and 6 months and between 6 and 12 months in the grafted sites, and additionally between 12 and 24 months in IBB sites. This significant RC decrease at the advanced healing stage was probably related to the prolonged presence of the IBB grafted particles and their continuing osteoconductivity, which contributed to the filling of the site.

In the β-TCP sites, the reduced size and decreasing morphologic change of the particles as observed between 3 and 6 months and 6 and 12 months was evidence of the material resorption phase. Only small fragments of β-TCP were present at 12 months. These fragments had been completely replaced by organized bone by 24 months. At the completely resorbed β-TCP sites, the regenerated tissue was more organized than the IBB sites at any time period. The slow resorption and continued

presence of the grafted IBB particles may have influenced and prolonged the bony remodeling process.

At 12 and 24 months, the healing site configuration was completely restored at all sites, whether membrane protected or uncovered. This could be attributed to the fact that these surgically created experimental intrabony defects were actually "4-wall defects." As such, the healing tissues were provided with excellent stability and optimal nourishment. However, the completely restored sites varied in content. While β-TCP particles were completely resorbed and the whole grafted site was occupied by regenerated osseous tissue, the "cancellous network" of the IBB-grafted site was composed of dense newly formed bone harboring a substantial amount of the grafted particles. The high osteoconductivity and the very slow resorptive pattern of IBB (assuming the particles are resorbed at all) could contribute to the strength of the newly formed cancellous network, upgrading the bone quality for future implant placement.

The biodegradability and resorption rate of the 2 biomaterials were totally different in the examined healing periods. The particle area fraction at the β-TCP sites progressively decreased until the particles were completely resorbed, while at the IBB sites, particle area fraction did not change significantly beyond 6 months. The fact that a statistically significant decrease of β-TCP particles was noted between 3 and 6 months, and especially between 12 and 24 months, showed that there was an accelerated resorptive phase in the later healing periods. Consequently, because of the continual β-TCP particle resorption, bone area fraction was significantly higher at the β-TCP sites than at IBB sites at 6, 12, and 24 months. Nevertheless, at the advanced healing periods, all grafted sites showed significantly smaller RC area fraction than control sites. It appears that the resultant healing site morphology was molded by these grafting materials. That is, the regenerated bone surface outline returned to its original contour in grafted sites.

Studies testing pure-phase β-TCP in vitro[30,42,43] in vivo in animal studies,[44–46] and more recently humans[23,47,48] have shown satisfactory results. Most studies using β-TCP in osseous deficiencies have shown high biocompatibility,[25–27] an influence on osteoconduction,[44,46,49] an association with osteoblastic activity,[50] and continuous osteoclastic resorption.[42,50–52] During the remodeling phase, β-TCP served as an agent for volume maintenance.[28,29] In experimental defects in miniature pig tibias,[45] β-TCP showed 90% to 95% particle resorption after 24 months, which is similar to the present observations.

β-TCP was completely resorbed after 24 months. Complete resorption of β-TCP was also shown in a comparative study in the spine.[51] Recently, this material was adopted for use in sinus augmentation procedures with a clinical outcome comparable to sinus augmented by autogenous bone.[23,47,53]

IBB has been widely used to generate bone growth in defective and/or deficient bone sites. The long-term presence of grafted particles has been reported in different augmented sites.[12,18–20,54–58] Although bovine bone mineral resorption is extremely slow, it has proved to be an excellent biocompatible and osteoconductive material.[7,8,16,18,59,60] In a recent study,[59] IBB in block form generated bone growth outside the original bone envelope, which demonstrates its excellence in terms of conduction. In an ultrastructural study,[22] bovine bone mineral showed a morphologic structure similar to that of human cancellous bone, primarily in terms of intercrystallite bonding.

Morphometric data[17,19,20,41,61–69] have shown an average of 15% to 30% area fraction occupied by the grafted IBB particles in an augmented site, depending on healing time observation and specimen retrieval location. Nevertheless, bone area fraction was similar to sites augmented by autogenous bone. The grafted particles actually occupied part of the area fraction usually occupied by soft tissue marrow. Furthermore, the long-lasting presence of the mineral particles completely incorporated with bone and strengthened the osseous tissue mass, creating a dense cancellous network, thus improving its biologic ability to withstand loading forces transmitted by implants placed in these sites. However, this should be further investigated before it is it is accepted as a conclusive finding. As well, controlled clinical human follow-up studies evaluating functional osseointegrated implants in these regenerated sites are warranted to test whether this structural "cancellous network" affects long-term success.

Certain limitations of the current animal model should be mentioned. The experimental defect was a nonpathologic basal bone site where chewing habits, functional forces, and saliva were not involved. However, several clinical implications could be drawn from the current findings. When an implant is placed in a regenerated ridge augmented by a nonautologous bone graft, 6 to 12 months are required to achieve optimal volumetric healing configuration. With IBB, it should be anticipated that at least 25% of the regenerated hard tissue will encase grafted particles. It appears that the long-term presence of the particles plays an important role in the hard tissue "cancellous network." The fact that osteoclasts were rarely seen raises the question of

whether the resorption mechanism of these grafting materials mimics the mechanism at work in the resorption of autogenous graft material. Another question that should be raised is the timing of implant placement in such a grafted site.

The present study demonstrated the advantages of the staged techniques over the simultaneous (bone augmentation and implant placement) technique. This finding is supported by other studies[70–72] using autogenous bone graft. As shown in this experimental design, placement of a protective membrane over this type of grafted intrabony site is unnecessary. However, a membrane is usually a *si qua non* in lateral and/or vertical regeneration procedures.

ACKNOWLEDGMENTS

The authors are grateful to The Lefcoe Fund for Research in Oral Biology and The Gerald A. Niznick Chair of Implant Dentistry (Incumbent, Prof H. Tal) for their support, to Dr Noam Kariv for animal care and maintenance, to Prof David M. Steinberg for his assistance in the statistical analyses, and to Ms Rita Lazar for editorial assistance.

REFERENCES

1. Fukuta K, Har-Shai Y, Collares MV, Lichten JB, Jackson IT. Comparison of inorganic bovine bone mineral particles with porous hydroxyapatite granules and cranial bone dust in the reconstruction of full-thickness skull defect. J Craniofac Surg 1992;3:25–29.
2. Isaksson S. Aspects of bone healing and bone substitute incorporation. An experimental study in rabbit skull bone defects. Swed Dent J 1992;84(suppl):1–46.
3. Klinge B, Alberius P, Isaksson S, Jonsson J. Osseous response to implanted natural bone mineral and synthetic hydroxylapatite ceramics in the repair of experimental skull bone defects. J Oral Maxillofac Surg 1992;50:241–249.
4. Hislop WS, Finlay PM, Moos KF. A preliminary study into the uses of anorganic bovine bone in oral and maxillofacial surgery. Br J Oral Maxillofac Surg 1993;31:149–153.
5. Thaller SR, Hoyt J, Borjeson K, Dart P, Tesluk H. Reconstruction of calvarial defects with anorganic barrier bone mineral in a rabbit model. J Craniofac Surg 1993;4:79–84.
6. Spector M. Anorganic bovine bone and ceramic analogs of bone mineral as implants to facilitate bone regeneration. Clin Plast Surg 1994;21:437–444.
7. Jensen SS, Aaboe M, Pinholt EM, Hjørting-Hansen E, Melsen F, Ruyter IE. Tissue reaction and material characteristics of four bone substitutes. Int J Oral Maxillofac Implants 1996;11:55–66.
8. Berghlundh T, Lindhe J. Healing around implants placed in bone defects treated with Bio-Oss. An experimental study in the dog. Clin Oral Implants Res 1997;8:117–124.
9. Hämmerle CHF, Chiantaella GC, Karring T, Lang NP. The effect of a deproteinized bovine bone mineral on bone regeneration around titanium dental implants. Clin Oral Implants Res 1998;9:151–162.
10. Artzi Z, Nemcovsky CE, Tal H. Efficacy of porous bovine bone mineral in various types of osseous deficiencies. Clinical observations and literature review. Int J Periodontics Restorative Dent 2001;21:395–405.
11. Dies F, Etienne D, Abboud NB, Ouhayoun JP. Bone regeneration in extraction sites after immediate placement of an e-PTFE membrane with or without a biomaterial. Report on 12 consecutive cases. Clin Oral Implants Res 1996;7:277–285.
12. Artzi Z, Nemcovsky CE. The application of deproteinized bovine bone mineral for ridge preservation prior to implantation. Clinical and histological observations in a case report. J Periodontol 1998;69:1062–1067.
13. Artzi Z, Tal H, Dayan D. Porous bovine bone mineral in healing of human extraction sockets. Part 1. Histomorphometric evaluation at 9 months. J Periodontol 2000;71:1015–1023.
14. Artzi Z, Tal H, Dayan D. Porous bovine bone mineral in healing of human extraction sockets. Part 2. Histochemical observations at 9 months. J Periodontol 2001;72:152–159.
15. Smiler DG, Johnson PW, Lozada JL, et al. Sinus lift grafts and endosseous implants: Treatment of the atrophic posterior maxilla. Dent Clin North Am 1992;36:151–186.
16. Wetzel AC, Stich A, Caffesse RG. Bone apposition onto oral implants in the sinus area filled with different grafting materials. A histological study in beagle dogs. Clin Oral Implants Res 1995;6:155–163.
17. Hürzeler MB, Quiñones CR, Kirsch A, et al. Maxillary sinus augmentation using different grafting materials and dental implants in monkeys. Part I. Evaluation of anorganic bovine-derived bone matrix. Clin Oral Implants Res 1997; 8:476–486.
18. Valentini P, Abensur D. Maxillary sinus floor elevation for implant placement with demineralized freeze-dried bone and bovine bone (Bio-Oss): A clinical study of 20 patients. Int J Periodontics Restorative Dent 1997;17:233–241.
19. Haas R, Donath K, Fodinger M, Watzek G. Bovine hydroxyapatite for maxillary sinus grafting: Comparative histomorphometric findings in sheep. Clin Oral Implants Res 1998;9: 107–116.
20. Artzi Z, Nemcovsky CE, Tal H, Dayan D. Histopathological morphometric evaluation of 2 different hydroxyapatite-bone derivatives in sinus augmentation procedures: A comparative study in humans. J Periodontol 2001;72:911–920.
21. Spector M. Basic principles of tissue engineering. In: Lynch SE, Genco RJ, Marx RE (eds). Tissue Engineering. Chicago: Quintessence, 1999:3–16.
22. Rosen VB, Hobbs LW, Spector M. The ultrastructure of anorganic bovine bone and selected synthetic hydroxyapatites used as bone graft substitute materials. Biomaterials 2002;23:921–928.
23. Szabo G, Suba Z, Hrabak K, Barabas J, Nemeth Z. Autogenous bone versus β-tricalcium phosphate graft alone for bilateral sinus elevations (2-and 3-dimensional computed tomographic, histologic, and histomorphometric observations): Preliminary results. Int J Oral Maxillofac Implants 2001;16:681–692.
24. Wiltfang J, Merten HA, Schlegel KA, et al. Degradation characteristics of alpha and β tri-calcium-phosphate (TCP) in minipigs. J Biomed Mater Res 2002;63:115–121.
25. Rosa AL, Brentegani LG, Grandini SA. Hydroxylapatite and tricalcium phosphate implants in the dental alveolus of rats. A histometric study. Braz Dent J 1995;6:103–109.
26. Hossain MZ, Kyomen S, Tanne K. Biologic responses of autogenous bone and beta-tricalcium phosphate ceramics transplanted into bone defects to orthodontic forces. Cleft Palate Craniofac J 1996;33:277–283.

27. Ohsawa K, Neo M, Matsuoka H, et al. The expression of bone matrix protein mRNAs around beta-TCP particles implanted into bone. J Biomed Mater Res 2000;52:460–466.
28. Breitbart AS, Staffenberg DA, Thorne CH, et al. Tricalcium phosphate and osteogenin: A bioactive onlay bone graft substitute. Plast Reconstr Surg 1995;96:699–708.
29. Gao TJ, Lindholm TS, Kommonen B, Ragni P, Paronzini A, Lindholm TC. Stabilization of an inserted tricalcium phosphate spacer enhances the healing of a segmental tibial defect in sheep. Arch Orthop Trauma Surg 1997;116:290–294.
30. Porter BD, Oldham JB, He SL, et al. Mechanical properties of a biodegradable bone regeneration scaffold. J Biomech Eng 2000;122:286–288.
31. Dong J, Uemura T, Shirasaki Y, Tateishi T. Promotion of bone formation using highly pure porous beta-TCP combined with bone marrow-derived osteo-progenitor cells. Biomaterials 2002;23:4493–4502.
32. Trisi P, Rao W, Rebaudi A, Fiore P. Histologic effect of pure-phase beta-tricalcium phosphate on bone regeneration in human artificial jawbone defects. Int J Periodontics Restorative Dent 2003;23:69–77.
33. Buser D, Hoffmann B, Bernard JP, Lussi A, Mettler D, Schenk RK. Evaluation of filling materials in membrane-protected bone defects. A comparative histomorphometric study in the mandible of miniature pigs. Clin Oral Implants Res 1998;9:137–150.
34. Karnovsky MJ. A formal dehydeglutaraldehyde fixture of high osmolarity for use in electron microscopy. J Cell Biol 1965;3:112–119.
35. Donath K, Breuner G. A method for the study of undecalcified bone and teeth with attached soft tissues. The Sage-Schliff (sawing and grinding) technique. J Oral Pathol 1982; 11:318–326.
36. Donath K. The diagnostic value of the new method for the study of undecalcified bones and teeth with attached soft tissue (Sage-Schliff sawing and grinding technique). Pathol Res Pract 1985;179:631–633.
37. Rohrer MD, Schubert CC. The cutting-grinding technique for histological preparation of undecalcified bone and bone-anchored implants: Improvement in instrumentation and procedures. Oral Surg Oral Med Oral Pathol 1992;74: 73–78.
38. Chalkey HW. Method for quantitative morphologic analysis of tissues. J Natl Cancer Inst 1943;4:47–53.
39. Bellhouse DR. Area estimation by point counting techniques. Biometrics 1981;37:303–312.
40. Ohnishi H, Fujii N, Futami T, Taguchi N, Kusakari H, Maeda T. A histochemical investigation of the bone formation process by guided bone regeneration in rat jaws. Effect of PTFE membrane application periods on newly formed bone. J Periodontol 2000;7:341–352.
41. Tarnow DP, Wallace SS, Froum SJ, Rohrer MD, Cho S-C. Histologic and clinical comparison of bilateral sinus floor elevations with and without barrier membrane placement in 12 patients: Part 3 of an ongoing prospective study. Int J Periodontics Restorative Dent 2000;20:116–125.
42. Yamada S, Heymann D, Bouler JM, Daculsi G. Osteoclastic resorption of calcium phosphate ceramics with different hydroxyapatite/beta-tricalcium phosphate ratios. Biomaterials 1997;18:1037–1041.
43. Tancred DC, McCormack BA, Carr AJ. A synthetic bone implant macroscopically identical to cancellous bone. Biomaterials 1998;19:2303–2311.
44. Saito M, Shimizu H, Beppu M, Takagi M. The role of beta-tricalcium phosphate in vascularized periosteum. J Orthop Sci 2000;5:275–282.
45. Merten HA, Wiltfang J, Grohmann U, Hoenig JF. Intraindividual comparative animal study of alpha- and beta-tricalcium phosphate degradation in conjunction with simultaneous insertion of dental implants. J Craniofac Surg 2001;12: 59–68.
46. Steffen T, Stoll T, Arvinte T, Schenk RK. Porous tricalcium phosphate and transforming growth factor used for anterior spine surgery. Eur Spine J 2001;10(suppl 2):S132–S140.
47. Scher EL, Day RB, Speight PM. New bone formation after a sinus lift procedure using demineralized freeze-dried bone and tricalcium phosphate. Implant Dent 1999;8:49–53.
48. Palti A, Hoch T. A concept for the treatment of various dental bone defects. Implant Dent 2002;11:73–78.
49. Cong Z, Jianxin W, Xingdong Z. Osteoinductivity and biomechanics of a porous ceramic with autogenic periosteum. J Biomed Mater Res 2000;52:354–359.
50. Knabe C, Driessens FC, Planell JA, et al. Evaluation of calcium phosphates and experimental calcium phosphate bone cements using osteogenic cultures. J Biomed Mater Res 2000;52:498–508.
51. Le Huec JC, Lesprit E, Delavigne C, Clement D, Chauveaux D, Le Rebeller A. Tri-calcium phosphate ceramics and allografts as bone substitutes for spinal fusion in idiopathic scoliosis: Comparative clinical results at four years. Acta Orthop Belg 1997;63:202–211.
52. Muschik M, Ludwig R, Halbhubner S, Bursche K, Stoll T. Beta-tricalcium phosphate as a bone substitute for dorsal spinal fusion in adolescent idiopathic scoliosis: Preliminary results of a prospective clinical study. Eur Spine J 2001;10 (suppl 2):S178–S184.
53. Chanavaz M. Sinus graft procedures and implant dentistry: A review of 21 years of surgical experience (1979–2000). Implant Dent 2000;9:197–206.
54. Clergeau LP, Danan M, Clergeau-Guerithault S, Brion M. Healing response to anorganic bone implantation in periodontal intrabony defects in dogs. Part I. Bone regeneration. A microradiographic study. J Periodontol 1996;67:140–149.
55. Skoglund A, Hising P, Young C. A clinical and histologic examination in humans of the osseous response to implanted natural bone mineral. Int J Oral Maxillofac Implants 1997; 12:194–199.
56. Schlegel AK, Donath K. Bio-Oss—A resorbable bone substitute? J Long Term Eff Med Implants 1998;8:201–209.
57. Young C, Sandstedt P, Skoglund A. A comparative study of anorganic xenogenic bone and autogenous bone implants for bone regeneration in rabbits. Int J Oral Maxillofac Implants 1999;14:72–76.
58. Schlegel AK, Fichtner G, Schultze-Mosgau S, Wiltfang J. Histologic findings in sinus augmentation with autogenous bone chips versus a bovine bone substitute. Int J Oral Maxillofac Implants 2003;18:53–58.
59. Araujo MG, Sonohara M, Hayacibara R, Cardaropoli G, Lindhe J. Lateral ridge augmentation by the use of grafts comprised of autologous bone or a biomaterial. An experiment in the dog. J Clin Periodontol 2002;29:1122–1131.
60. Schmitt JM, Buck DC, Joh SP, Lynch SE, Hollinger JO. Comparison of porous bone mineral and biologically active glass in critical-sized defects. J Periodontol 1997;68:1043–1053.
61. McAllister BS, Margolin MD, Cogan AG, Buck D, Hollinger JO, Lynch SE. Eighteen-month radiographic and histologic evaluation of sinus grafting with anorganic bovine bone in the chimpanzee. Int J Oral Maxillofac Implants 1999;4:361–368.
62. Valentini P, Abensur D, Wenz B, Peetz M, Schenk R. Sinus grafting with porous bone mineral (Bio-Oss) for implant placement: A 5-year study on 15 patients. Int J Periodontics Restorative Dent 2000;20:245–253.

63. Hanisch O, Lozada JL, Holmes RE, Calhoun CJ, Kan JY, Spiekermann H. Maxillary sinus augmentation prior to placement of endosseous implants: A histomorphometric analysis. Int J Oral Maxillofac Implants 1999;14:329–336.
64. Piattelli M, Favero GA, Scarano A, Orsini G, Piattelli A. Bone reactions to anorganic bovine bone (Bio-Oss) used in sinus procedures: A histologic long-term report of 20 cases in humans. Int J Oral Maxillofac Implants 1999;14:835–840.
65. Terheyden H, Jepsen S, Moller B, Tucker MM, Rueger DC. Sinus floor augmentation with simultaneous placement of dental implants using a combination of deproteinized bone xenografts and recombinant human osteogenic protein-1. A histometric study in miniature pigs. Clin Oral Implants Res 1999;10:510–521.
66. Yildirim M, Spiekermann H, Biesterfeld S, Edelhoff D. Maxillary sinus augmentation using xenogenic bone substitute material Bio-Oss in combination with venous blood: A histologic and histomorphometric study in humans. Clin Oral Implants Res 2000;11:214–229.
67. Artzi Z, Nemcovsky CE, Dayan D. Bovine-HA spongiosa blocks and immediate implant placement in sinus augmentation procedures. Histopathological and histomorphometric observations on different histological stainings in 10 consecutive patients. Clin Oral Implants Res 2002;13:420–427.
68. Hallman M, Lundgren S, Sennerby L. Histologic analysis of clinical biopsies taken 6 months and 3 years after maxillary sinus floor augmentation with 80% bovine hydroxyapatite and 20% autogenous bone mixed with fibrin glue. Clin Implant Dent Relat Res 2001;3:87–96.
69. Hallman M, Hedin M, Sennerby L, Lundgren S. A prospective 1-year clinical and radiographic study of implants placed after maxillary sinus floor augmentation with bovine hydroxyapatite and autogenous bone. J Oral Maxillofac Surg 2002; 60:277–284.
70. Jensen OT, Sennerby L. Histologic analysis of clinically retrieved titanium microimplants placed in conjunction with maxillary sinus floor augmentation. Int J Oral Maxillofac Implants 1998;13:513–521.
71. Lundgren S, Rasmusson L, Sjostrom M, Sennerby L. Simultaneous or delayed placement of titanium implants in free autogenous iliac bone grafts. Histological analysis of the bone graft–titanium interface in 10 consecutive patients. Int J Oral Maxillofac Surg 1999;28:31–37.
72. Rasmusson L, Meredith N, Cho IH, Sennerby L. The influence of simultaneous versus delayed placement on the stability of titanium implants in onlay bone grafts. A histologic and biomechanic study in the rabbit. Int J Oral Maxillofac Surg 1999;28:224–231.